Title

Predicting soil permanganate oxidizable carbon (POXC) by coupling DRIFT spectroscopy and artificial neural networks (ANN)

Authors

Margenot, Andrew
Neill, Terry O'
Sommer, Rolf
et al.

Publication Date

2020

DOI

10.1016/j.compag.2019.105098

Peer reviewed

Computers and Electronics in Agriculture 168 (2020) 105098

Contents lists available at ScienceDirect

Computers and Electronics in Agriculture

journal homepage: www.elsevier.com/locate/compag

Original papers

Predicting soil permanganate oxidizable carbon (POXC) by coupling DRIFT spectroscopy and artificial neural networks (ANN)

Andrew Margenot[a,*], Terry O' Neill[b], Rolf Sommer[c], Venkatesh Akella[b]

[a] Department of Crop Sciences, University of Illinois Urbana-Champaign, Urbana, IL 61801, USA
[b] Department of Electrical & Computer Engineering, University of California Davis, Davis, CA 95616, USA
[c] International Center for Tropical Agriculture, P.O. Box 823-00621, Nairobi, Kenya

ARTICLE INFO

Keywords:
Infrared spectroscopy
Partial least square regression
Artificial neutral networking
Soil carbon
Kenya

ABSTRACT

Infrared spectroscopy has transformed soil property quantification by enabling low-cost, high-throughput analysis of soils, enabling mapping and monitoring of this non-renewable resource. However, less evaluated are newly emerging indicators of soil health. Furthermore, as soil spectral libraries expand in size, commonly employed linear models such as partial least squares regression (PLSR) may be challenged by the number and diversity of spectra. Artificial neural networks (ANN) are an emerging deep learning approach that can offer advantages in quantification of soil properties by utilizing non-linear relationships among spectra and soil components. We compared ANN versus PLSR models for predicting an increasingly used soil health indicator, permanganate oxidizable C (POXC), as well as more routinely predicted soil variables (e.g., clay, soil organic C [SOC]), across a gradient of soil organic matter furnished by a deforestation chronosequence in Kenya (n = 144). Candidate ANN architectures were first methodologically evaluated and described to identify best-practices for the application of ANN to soil spectroscopy. Predictions by the resulting ANN relative to PLSR were similar or slightly improved for routinely measured variables that represent soil organic matter (SOC, C:N) and physical properties (clay, silt, sand, bulk density). The accuracy of POXC predictions were similar for ANN (RMSE 102 mg kg^{-1}) and PLSR (RMSE 106 mg kg^{-1}). However, models drew on shared but also distinct wavenumbers, indicating differential use of information in soil infrared spectra by non-linear versus linear chemometric models. Even in relatively small spectral datasets of similar soil types expected to favor PLSR, ANN shows comparable predictive performance. To help guide future applications of ANN in soil spectroscopy, we propose a systematic procedure to select ANN model hyperparameters.

1. Introduction

Infrared spectroscopy is driving a global revolution in the mapping and monitoring of soil, a non-renewable resource that provisions multiple services to human societies (Nocita et al., 2015). Chemometric prediction is increasingly employed for determining relatively static soil variables such as texture and total soil organic matter (SOM), (Viscarra Rossel et al., 2016) but the ability of infrared spectroscopy to predict sensitive and therefore temporally variable indicators of SOM dynamics has been less evaluated. Developing chemometric models to quantify general soil properties is well established (Bellon-Maurel et al., 2010) and is increasingly applied to quantify SOM fractions (Calderón et al., 2017; Peltre et al., 2014; Zhang et al., 2017). Chemometric predictions employing diffuse reflectance infrared Fourier transform (DRIFT) spectra in the mid-infrared (MIR; 4000 – 400 cm^{-1}) and/or near-infrared (NIR; 12,000–4000 cm^{-1}) offer a robust, low-cost, and rapid alternative to traditional wet chemical analyses of SOM fractions used to assess nutrient cycling, soil C stabilization, and soil health. In developing nations in which technical capacity and costs constrain traditional soil analyses, chemometric predictions of soil properties enabled by DRIFT spectroscopy have transformed soil assessment and enabled local to continental soil mapping (e.g., African Soil Information Service (AfSIS) (Liu et al., 2018). However, soil health variables remain less evaluated globally and in particular in developing nations (Berazneva et al., 2018). An emerging soil health variable that is also an SOM fraction is permanganate oxidizable C (POXC), which has been proposed to be an early indicator of SOM accrual (Hurisso et al., 2016; Lucas and Weil, 2012) and to reflect soil C mineralization and stabilization processes sensitive to microbial activity (Hurisso et al., 2016; Paul et al., 2013; Schindelbeck et al., 2016).

* Corresponding author.
E-mail address: margenot@illinois.edu (A. Margenot).

https://doi.org/10.1016/j.compag.2019.105098
Received 18 May 2019; Received in revised form 30 September 2019; Accepted 6 November 2019
Available online 04 December 2019

DRIFT spectroscopy-based predictions of soil variables can achieve a degree of repeatability and/or precision comparable or greater than traditional wet chemistry analyses (Shepherd et al., 2005), though the accuracy of chemometric predictions can vary widely depending on the soil variable(s) of interest, soil type, sample size, and chemometric models (Viscarra Rossel et al., 2006). Coupling DRIFT spectroscopy and chemometrics enables sample throughput rates of up to several hundred per day (Reeves III et al., 2012). This enables detailed monitoring or mapping of soil C and related soil properties at field, landscape, continental, and global scales (Nocita et al., 2015; Sanchez et al., 2009; Stevens et al., 2013). Several efforts are currently underway to build soil spectral libraries of national (Castaldi et al., 2018; Wijewardane et al., 2016b) and global coverage (Viscarra Rossel et al., 2016).

Partial-least squares regression (PLSR) is a linear model commonly employed in chemometric predictions of soil variables from DRIFT spectra. While PLSR is suitable for similar soil types (e.g., mineralogy, particle size) (Reeves III and Smith, 2009; Stumpe et al., 2011), accurate PLSR prediction of soil variables that constitute a minor component of DRIFT spectral absorbances such as SOM fractions may be challenged. On a limited soil sample set (n = 24) encompassing a gradient of POXC (550 to 1430 mg kg^{-1}) induced by long-term management on a single soil type, Veum et al. (2014) demonstrated decent prediction accuracy of POXC from MIR using PLSR (R^2 = 0.69, RMSEV = 220 mg kg^{-1}) and higher prediction accuracy with VNIR (R^2 = 0.94, RMSEV = 120 mg kg^{-1}). However, spectra were collected on demineralized (hydrofluoric acid-treated) soil samples, a laborious soil pre-treatment not commonly practiced for high-throughput spectral analyses and also prone to artifacts (Margenot et al., 2017; Yeasmin et al., 2017). Using a larger and more edaphically diverse soil sample set across the United States (n = 496), acceptable prediction of POXC from MIR spectra using PLSR, has been achieved (e.g., up to R^2 = 0.81, RMSEV = 144 mg kg^{-1}) and with better prediction of POXC using MIR compared to NIR Calderón et al. (2017).

The artificial neural network (ANN) is a non-linear, non-parametric model that has dramatically risen in prominence within the machine learning community over the past six years (Liu et al., 2017) and has seen recent application to soil science for digital mapping (Bagheri Bodaghabadi et al., 2015; Were et al., 2015) and spectral predictions of soil variables (Morellos et al., 2016; Wijewardane et al., 2016b). The salient advantage of ANN is its use of non-linear relationships between the measured data and the predicted properties. Because an ANN may be able to address non-linear spectral responses better than PLSR, it has been leveraged to improve accuracy of predictions in multiple applications and disciplines, including quantifying variables from spectra (Zhao et al., 2006).

Large-scale comparisons of ANN and PLSR for prediction of soil properties (e.g., clay) from infrared spectra have found ANN to outperform PLSR using a global model of relatively large datasets (n > 20,000) but the opposite has been found for local models and/or smaller datasets (Rossel and Behrens, 2010; Wijewardane et al., 2016a; Wijewardane et al., 2016b). However, the relative performance of ANN and PLSR for soil spectra-based predictions using local datasets (i.e., edaphically homogenous) appear to be specific to the soil variable. For example, ANN had comparable prediction as PLSR for soil organic C (SOC) but not for labile inorganic nutrient element fractions across fields in Belgium and northern France (n = 168) (Mouazen et al., 2010).

To evaluate the potential of ANN to support high-throughput soil health assessments, we utilized a geographically constrained dataset considered 'local' by virtue of similar soil type and relatively small size (n = 144) to conservatively test the hypothesized advantage of the non-linear model of ANN relative to PSLR for chemometric prediction of POXC, a labile SOM fraction and minor mass component of soil (generally < 0.2%), from DRIFT spectra of soils. The specific research objectives were to:

(i) Explore ANN architectures to determine a suitable network design for use with soil DRIFT spectra;
(ii) Evaluate the accuracy of PLSR compared to ANN to predict POXC;
(iii) Identify organic and mineral function groups in soils associated with POXC by examining infrared frequencies used in PLSR vs ANN models of POXC; and
(iv) Evaluate the applicability of an ANN architecture selected for efficacy in predicting one soil variable to be trained for another soil variable, specifically for POXC-based architectures to be used to predict variables routinely predicted with PLSR (e.g., clay, SOC).

2. Materials & methods

2.1. Site description

Soils were sampled from the Nandi forest and adjacent agricultural fields in Nandi County, Kenya. The Nandi forest is a remnant of the formerly contiguous Guineo-Congolian rainforest, and one of the few relic primary rainforests remaining in East Africa (Lehmann et al., 2007) since the expansion of agriculture in this region in early 20th century (Solomon et al., 2007). The Nandi forest is composed of a mixture of Guineo-Congolian species such as *Aningeria altissima*, *Milicia excelsa*, *Antiaris toxicaria*, *Chrysophyllum albidum* (Solomon et al., 2007). Sites were situated at 1700–1800 m above sea level, with a mean annual temperature of 19 °C and mean annual precipitation estimated at 2000 mm (Solomon et al., 2007). Soils are developed from biotite-gneiss parent materials and are classified as Hapludoxes (USDA Taxonomy) or as Humic Nitosols (FAO) (Lehmann et al., 2007). In addition to primary forest (n = 4), agricultural fields (n = 20) of varying time of establishment from the forest were sampled in March 2017 to furnish a gradient of SOC and POXC across similar soil mineralogy and texture. At each site (n = 24 total), soils in three sub-plots were sampled by augur at 0 – 20 cm and 20 – 40 cm depths for a total of n = 144 soil samples. Soils were air-dried prior to analyses.

2.2. Soil analyses

Dry soils were gently crushed to pass a 2 mm sieve. Soil texture was determined by laser diffraction particle size analysis (LDPSA) across a size range of 3000 – 0.01 μm using a Horiba LA-950V2 (Horiba Ltd., Kyoto, Japan) (Towett et al., 2015). Suspended soil samples were analyzed following dispersion by sonication (130 W, 20 kHz). Total soil organic C (SOC) and nitrogen (TSN) was determined as total soil C using a CN elemental analyzer (Elementar, Hanau, Germany). Permanganate oxidizable carbon (POXC) was determined based on Weil (2003) as modified by Culman (2012) using 0.02 mol L^{-1} $KMnO_4$. Non-reduced Mn^{7+} was quantified by colorimetry (550 nm) and POXC was calculated assuming the oxidation of 9000 mg C per mol Mn^{7+} reduced (Weil et al., 2003).

2.3. DRIFT spectroscopy

Soils were analyzed by DRIFT spectroscopy by collecting spectra in the MIR region and part of the NIR region (7500–600 cm^{-1}), as is standard for many soil spectroscopic characterizations (Viscarra Rossel et al., 2006), using a Tensor 27 HTS-XT spectrometer (Bruker, Brennen, Germany). Sieved soils (< 2 mm) were subsampled by coning and quartering, and ground to < 0.5 mm using a RM 200 Restch motor grinder. The resulting finely ground soil samples were loaded into stainless steel wells and surface-leveled. Duplicate spectra were collected for each soil.

Duplicate spectra were evaluated for outliers prior to PLSR and ANN using The Unscrambler X, V10.4 (Camo Inc., Oslo, Norway) using principal component analyses (PCA) to visualize variability in spectra (Calderón et al., 2017; Guillou et al., 2015). To test for potential outliers, Mahalanobis distance analysis was used with an elliptical decision

boundary ($p < 0.05$) as well as Hotelling's T^2 (Calderón et al., 2017). One outlier replicate spectrum characterized by high leverage was identified by both tests and removed. For all other soils, duplicate spectra were averaged to obtain one mean spectrum per soil sample ($n = 144$).

2.4. Partial least squares regression (PLSR)

Prediction of POXC from DRIFT spectra was first performed using PLSR. To enable direct comparison of PLSR and ANN, a PLSR model was developed using the same open source software and libraries as was used for ANN: Python 3.6 and scikit-learn (Pedregosa et al., 2011). This was done to validate the computation environment and data import from the proprietary format OPUS spectroscopy for use in the neural network research outlined below. PLSR model performance was evaluated for fit (R^2) and accuracy (RMSE) of POXC predictions. Exploration of the number of components most appropriate for a POXC regression model was performed by varying the number of components used. First, 80% of the dataset observations were randomly selected as the calibration set, and the remaining 20% was withheld for independent validation (Calderón et al., 2017; Nanni et al., 2018; Xie et al., 2015). For each train-validation split, a PLSR model was built for component counts from 2 to 30, a range of components chosen to bound component variation from what is likely too few to unnecessarily high number of components and thus risks overfitting (Rossel and Behrens, 2010). This calibration was performed for a total of 50 different, randomized splittings of the data into training and validation sets. Mean RMSE and R^2 were calculated using model performance for $n = 50$ splits.

2.5. Artificial neural networks (ANN)

2.5.1. Background on ANN

An artificial neural network (ANN) consists of three components: an input layer, a series of one or more hidden layers and a regression layer (Fig. 1). The hidden layers are composed of neurons, the basic computation unit of a neural network. A neuron receives inputs from the previous layer, scales each input by a weight, adds a bias and then applies an activation function to the result. The output of each individual neuron is thus: $\boldsymbol{F_{activation}}(\sum \boldsymbol{w_i x_i} + \boldsymbol{b})$.

The activation function serves to de-linearize the function approximated by the ANN. Popular activation functions include sigmoid, $\boldsymbol{\sigma(x)} = \frac{1}{(1+e^{-x})}$, hyperbolic tangent, $\boldsymbol{tanh(x)} = \frac{e^x - e^{-x}}{e^x + e^{-x}}$, and Rectified Linear Unit (ReLU), relu(x) = maximum(0,x). The output of each neuron is passed to all, or some subset of, the neurons in the subsequent layers. In this way a neural network can be formed by linking many neurons together in multiple layers. This allows the neural network to act as function approximator for complex functions. Increasing the number of neurons and layers allows for approximation of increasingly complex function.

In the case of the final hidden layer, all outputs are passed to a regression layer for final estimation. Generally, the collection of weights and biases of the network are referred to as the *parameters*. Other details, such as the numbers of neurons in each layer, the number of layers, the activation function, and how the neurons are connected, are referred to as the *hyper-parameters* of the network.

The training of an ANN consists of exposing the network to the training data until (i) the network approximates the function it is intended for or (ii) no further improvement can be achieved. The network is exposed to the training data in small batches. After each batch, the parameters are adjusted in a way that ensures a more accurate output from the network for that batch. The process of exposing the network to training data in batches and then updating the parameters is repeated until the training set is complete. Exposing the entire training set to the network is considered one epoch. Usually the training set is exposed to the network for multiple epochs before training is complete. For large datasets fewer epochs are needed whereas for small datasets more epochs are necessary, increasing the risk of over-fitting.

2.5.2. ANN architecture and hyper-parameter selection

We began exploration of ANN architecture with networks similar to the large, deep ANN used in image classification. These networks, often with thousands of neurons in each layer and millions of parameters per network (Real et al., 2017; Szegedy et al., 2015), were unnecessarily complex and difficult to train with our comparatively small dataset of soil spectra ($n = 144$). In most popular applications, ANN are trained with larger datasets commonly $n > 10{,}000$, though ANN can be succesfully used on small datasets ($n > 100$) (Tange et al., 2017). Given the reduced input dimensionality of the spectral data (absorbance intensity at 3578 frequencies across 7500–600 cm^{-1}) and relatively small dataset ($n = 144$) a small network was considered most appropriate. The following network hyper-parameters and training parameters were varied in explorations:

(i) Number of Hidden Layers in the ANN. Networks were tested with 1, 2, 3, 5, 10, and 20 hidden layers.
(ii) Number of neurons in the hidden layers. This was varied from 10 to 100 in increments of both 3 and 5, depending upon the number of layers used. These increments were chosen for expediency (to reduce computation time) and becaus they were small enough to monitor when network improvements occurred.
(iii) Symmetry of hidden layers (variable number of neurons between

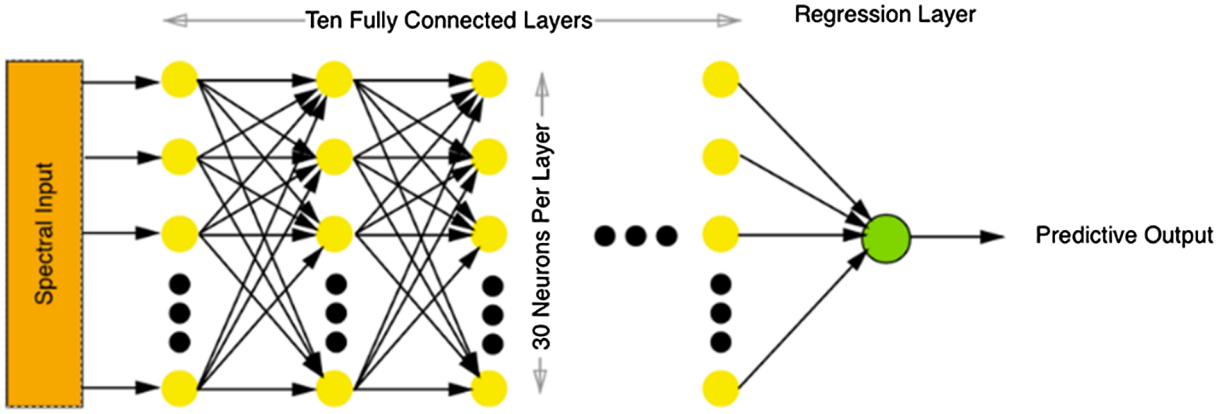

Fig. 1. Schematic of artificial neural networking (ANN) for prediction of soil variables (e.g., permanganate oxidizable carbon [POXC]) from diffuse reflectance infrared Fourier transform (DRIFT) spectra of soils. Spectral input included combined NIR and MIR spectra (7500–400 cm^{-1}) or truncated spectra (e.g., 1800–400 cm^{-1}).

layers). This was done mainly with 2-layer networks, and with the second layer varying from equaling the size of the first hidden layer down to approximately half the number of neurons.

(iv) Batch size used during batch-gradient descent phase of ANN training. This was varied in powers of two from 1 to 64. This is the number of data sample the network is exposed to before making modifications to the network in an attempt to improve the model. Smaller batches sizes are more computationally intense, and thus take longer to train the network, but more can be learned from each sample. Large batches sizes require less computation but learning can be slower and subtleties found in individual samples can be missing in training.

(v) Number of training epochs. This was also varied in exponents of two from 1 to 2048, with further refinement after the likely a point of over fitting was discovered.

(vi) Activation Function. This was tested with the ReLU, hyperbolic tangent, and sigmoid functions. The activation function is what allows the ANN to 'learn' a non-linear model (Abadi et al., 2016).

After preliminary ad-hoc testing of various networks, a systematic approach was adapted. The initial exploration was performed to provide a large potential architectural design space. Determining which configurations were outside feasibility, insufficient or over-designed allowed us to limit the design exploration and select a design space that seemed promising. Adopting an iterative approach or a heuristic method to explore potential models is needed, not unlike the iterative testing of PLSR models developed by various methods such as spectral preprocessing and on selected spectral regions (e.g., Calderón et al., 2017). The systematic approach used is outlined below. Among the first observation made during speculative testing was that the activation function had little effect on model prediction accuracy. As such the ReLU was used exclusively afterward as its simplicity reduces computation time and shortens training and testing time (Abadi et al., 2016).

The basic kernel of testing is:
For each parameter variation{
Train a network using 10 different ways train- validation splits.
}
Record the outcomes.
The search heuristic:
Select a single ANN near the middle of design space.
For some small number of iterations {
Vary Epoch and Batch size and perform the basic kernel.
(In the first iteration these should be varied broadly)
Limit the Epoch and Batch to a small range that worked best.
Expand the number of Network layers and Neurons in the ANN to be explored.
(Both reducing and expanding the number of layers and neurons)
Perform the basic Kernel.
Limit the Kernel and Layers size to a small range that worked best
}

For several more iterations, select some another ANN some distance from the previously selected design and begin again.

After multiple iterations, the most promising ANN can be tested and trained for a greater number of train-validation splits to accurately assess the model reliability and performance (e.g., RMSE of POXC prediction).

2.5.3. ANN model calibration and validation

Soil spectra were independently used to develop ANN model for prediction of POXC. The same randomly sub-sampled dataset used to calibrate (80% of data) and then independently validate (20%) the PLSR model was used to enable comparability of PLSR and ANN model results. The entire dataset was randomly split into a training (80% of data) and test set (20% of data). ANN and PLSR models were calibrated using the same training set and validated using the same test set. To account for variable performance with different data splits, the data was split in ten different iterations, in which PLSR and ANN models were trained and tested in ten separate instances.

The hyper-parameters that determine ANN architecture (Fig. 1) and that were explicitly tested during ANN development for soil variables were:

(i) Number of hidden layers
(ii) Number of neurons in the hidden layers
(iii) Batch size used during batch-gradient descent phase of training
(iv) Number of training epochs
(v) Activation function

All ANN exploration was performed using open source tools. Python 3.6 was used as the development environment (Chollet, 2015) for high level model description and TensorFlow (Abadi et al., 2016) was used as the backend computational library. Over 6000 architectures and hyper-parameter combinations were explored to determine one suitable for POXC estimation. The final architecture used was an ANN with an input layer of the spectral data, ten hidden layers each using a rectified linear unit activation function, and a single regression layer for output. Each hidden layer was fully connected and contained 30 neurons (Fig. 1). The network was trained for 384 epochs using a batch size of 2. After this architecture and hyper-parameter combination was empirically selected as the most promising, a final analysis was performed. The ANN was trained and tested by splitting the data into a training and validation set. A total of 50 different train-validation splits were performed. Minimal data preprocessing was performed before network training and testing. In brief, each frequency of the spectral input data was standardized by removing the mean and scaling to unit variance. Spectra were not further processed (i.e., spectral pre-processing treatment such as normalization or baseline correction) because the hypothesized advantage of ANN over PSLR is robustness in accounting for input (i.e., spectra).

The selected network was also trained and tested with various subsets of the spectra sampled. To test ANN vs PLSR prediction resilience to limited spectral information, spectra were reduced by sampling every n^{th} wavenumber across three orders of magnitude of reduction: n = 1, 2, 3, 5, 10, 15, 30, 50, 100. Model performance was separately testing using limited portions of the spectrum: (1) the alcohol O-H, amine N-H, and aliphatic C-H region at 4405–3100 cm^{-1}; and (2) the region of absorbance by organic and mineral moieties hypothesized to be related to this labile C fraction (Calderón et al., 2017; Margenot et al., 2017) at 3700–3600 cm^{-1} and 1800–1000 cm^{-1}. These two regions were proposed by Calderón et al. (2017) to offer comparable predictions as the full MIR (4000–400 cm^{-1}). PLSR and ANN models were trained and tested in the manner described previously. To ensure that the minimum sufficient amount of spectral data necessary for PLSR compared to ANN, a 2-layer neural network and 10 component PLSR model were trained using increasingly large subsets of the complete dataset, from n = 1 to n = 80 spectra using twenty different train-validation splits for each training set size. PLSR and ANN showed similar improvement of RMSE for POXC up until n = 60 spectra were used, after which no improvement (lower RMSE) was detected.

Finally, the suitability of the architecture developed for the ANN model for POXC to predict additional soil properties, also considered soil health indicators, was tested. The same architecture and hyper-parameter combination for POXC was used to train ANN to predict bulk density, SOC, total nitrogen (TSN), carbon to nitrogen ratio (C:N), β-glucosidase activity, and particle size fractions of clay, silt, and sand. As with POXC, β-glucosidase activity is considered a newly emerging biological indicator of soil health, whereas the remaining variables are considered soil health physical indicators (bulk density, clay, silt, sand) or chemical indicators (SOC, TSN, C:N) (NRCS, 2019; SHI, 2017). To enable comparison of PLSR and ANN, separate PLSR models were developed in the same manner as for POXC for these additional soil

variables. The RMSE of validations and R^2 were reported for all predictions for further comparison of ANN and PLSR

2.6. Evaluation of wavenumbers used for chemometric models

Evaluating specific wavenumbers used by chemometric models can be used to evaluate functional relationships between the spectral input with the predicted analyte (Roggo et al., 2007). For PLSR, inspection of component loadings enables identification of specific wavenumbers that are related indirectly or directly to the soil variable predicted since these wavenumbers were used by the model for prediction (Calderón et al., 2017). In contrast, ANN is generally considered a 'black box' in that it does not offer direct evaluation of the functional relationships between input (i.e., spectra) and predicted variables (e.g., POXC) (Were et al., 2015), because every instance calculated by the network entails a distinct valuation of input. However, it is possible to visualize wavenumber loadings for particular instance(s) of the ANN model. Since an ANN is given no initial indication as to which wavenumbers are likely to contain relevant information, it discovers a set of wavenumbers stochastically which can be used for regression. We trained four neural networks with a single hidden layer to examine the wavenumbers were weighted heavily by the network, and thus were more likely to be relevant to POXC. We then selected the highest weight assigned to every wavenumbers for each instance and plotted them. The resulting plots for each ANN trained show which wavenumbers the network discovered could be used to predict POXC. These ANN were developed solely to observe the wavenumbers used and to demonstrate that there are multiple different wavenumbers groupings that can be used to infer POXC.

3. Results and discussion

3.1. Soil properties

POXC was generally highest under forest and lowest under agricultural use (Table 1). Greatest variability in POXC for cultivated sites occurred for 50 y agricultural fields (n = 5), ranging from 1197 ± 38 mg kg^{-1} to 470 ± 181 mg kg^{-1}. Younger and older agricultural fields with the same chrono-replication exhibited lower variability. POXC was positively correlated with TSC (R^2 = 0.75, $p < 0.0001$). Across sites, variation in POXC (8.8-fold) was less than total SOC (13.9-fold) but more than β-glucosidase activity (6.7-fold). Soil textural class varied from clay to sandy clay loam, with clay content ranging from 26 to 91%.

3.2. PLSR and ANN prediction of POXC

Using the full spectrum collected (8000–600 cm^{-1}), the PLSR model predicted POXC with an accuracy (RMSE) of 106 mg kg^{-1} using 50 different train-validation splits (Table 2). An increase in PLSR predictive accuracy (lower RMSE) occurred until 9 components were used, after which an increase in components yield little change in RMSE, which decreased with ≥ 20 components. The ANN architectures tested exhibited acceptable prediction of POXC with a performance similar to that of PLSR (Table 2). A few showed promise of performing better than PLSR when tested for a small number of train-test splits. The selected ANN (see Section 2.5) predicted POXC with slightly greater (+3.9%) accuracy than PLSR (−4 mg kg^{-1} RMSE).

Model accuracy was tested using reduced spectra in which every n^{th} wavenumber from n = 2 to 100. Accuracy of POXC predictions (RMSE) by PLSR and the ANN exhibited resilience to spectral reduction (Table 3). Prediction accuracy of ANN slightly increased with spectral reduction but was similar for PLSR. For example, spectral reduction to every 50th wavenumber led lowered RMSE of ANN from 102 to 95 mg kg^{-1} and of PLSR from 106 to 105 mg kg^{-1}.

Table 1
Descriptive statistics of soil properties evaluated for prediction by artificial neural networking (ANN) compared to partial least squares regression (PLSR) for soils from a deforestation chronosequence in Nandi County, western Kenya (n = 144).

	Mean	Median	Min	Max
Clay (%)	29.5	27.9	13.6	49.2
Silt (%)	19.9	20.0	7.6	28.0
Sand (%)	50.7	50.4	32.4	76.4
Bulk density (g cm^{-1})	1.02	1.01	0.71	1.53
SOC (g kg^{-1})	36.1	35.3	6.1	85.0
C:N	9.7	9.8	5.7	12.0
POXC (mg kg^{-1})	749	737	157	1382
β-glucosidase (μmol *p*NP g^{-1} h^{-1})	0.79	0.77	0.27	1.82

Table 2
Summary of previous POXC predictions from diffuse reflectance infrared Fourier transform (DRIFT) spectra of soils.

Study	Veum et al 2014		Calderón et al. 2017	This study	
Sample size (n)	24		496	144	
Scale	Field		Continental	Regional	
Method	PLSR	MLR	PLSR	PLSR	ANN
R^2	0.69	0.83	0.77	0.75	0.77
RMSE (mg kg^{-1})	220	150	144	106	102

3.3. Differential use of infrared absorbances by PLSR vs ANN models for POXC

Infrared frequencies used by PLSR (Fig. 2) and ANN (Fig. 3) were examined to assess which functional groups of mineral and organic matter phases were driving chemometric determination of POXC. The four randomly selected instances of the ANN demonstrate that similar wavenumbers were being employed, and that these largely corresponded to inorganic (mineral) functional groups, notably phyllosilicate O-H at 3697 – 3624 cm^{-1}, quartz-like Si-O at 2050 – 1780 cm^{-1}, and Fe-O, Al-O, and Si-O at 927 – 818 cm^{-1}. Wavenumbers corresponding to organic functional groups were less strongly weighed than those of mineral functional groups, and were strongest for aliphatic C-H at 2920 and 2852 cm^{-1}, aromatic C = C at 1593 cm^{-1}, and a mixture of phenol, carboxyl, and ester C-O at 1333 – 1034 cm cm^{-1}. Contribution of absorbances in the NIR (7500 – 4000 cm^{-1}) to ANN were negligible in all four instances.

3.4. Architectural transfer to other soil properties

The ANN architecture developed for POXC exhibited high transferability for other variables, with comparable or better prediction of additional soil variables relative to predictions by PLSR models developed separately for each additional soil variable (Table 3). ANN generally performed better than PLSR at predicting additional soil properties, as indicted by lower mean RMSE (-Δ). PLSR yielded greater prediction accuracy for soil bulk density and β-glucosidase activity relative to ANN, whereas SOM related variables SOM (SOC, TSN, C:N) and texture (clay, sand, silt) were predicted with greater accuracy using ANN. Though predicted using an architecture developed for POXC, total SOC showed the greatest difference in more accurate predictions by ANN compared to PLSR (-35% RMSE).

4. Discussion

4.1. POXC and SOM prediction by PLSR vs ANN

Inference of soil variables using ANN compared favorably with PLSR despite the use of a relatively small and edaphically homogenous

Table 3
Comparison of artificial neural networking (ANN) and partial least-squares regression (PLSR) for prediction of soil variables from DRIFT spectra.

Variable	ANN RMSE	PLSR RMSE	ANN R^2	PLSR R^2	ANN RPD	PLSR RPD	ANN SD	PLSR SD
Clay (%)	3.5	3.9	0.78	0.78	1.95	2.04	6.8	7.9
Sand (%)	3.4	3.4	0.83	0.79	2.35	2.40	7.9	8.2
Silt (%)	2.3	2.6	0.64	0.65	1.77	1.56	4.0	4.0
Bulk density (g cm^{-3})	0.11	0.10	0.52	0.60	1.46	1.26	0.16	0.13
SOC (g kg^{-1})	0.35	0.54	0.92	0.84	3.13	2.16	1.10	1.17
C:N	0.43	0.50	0.76	0.71	2.36	1.86	1.01	0.93
POXC	106	102	0.77	0.75	2.10	2.00	223	204
β-glucosidase (μmol pNP $g^{-1}h^{-1}$)	0.23	0.20	0.52	0.52	1.14	1.08	0.26	0.22

RMSE, root mean square error; RPD, ratio of performance to deviation; SD, standard deviation.

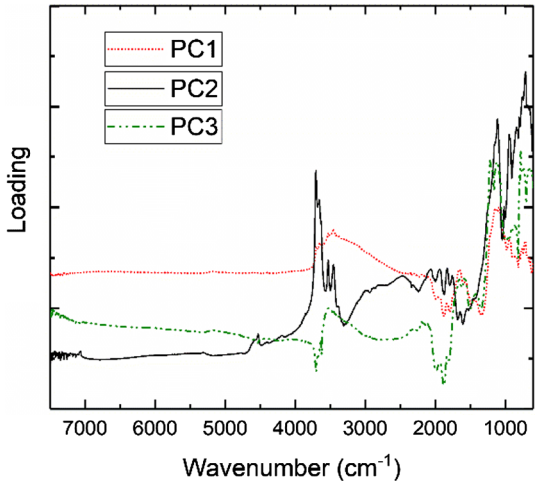

Fig. 2. Component loadings of partial least square regression (PLSR) model for prediction of POXC for soils in western Kenya (n = 144) using DRIFT spectroscopy.

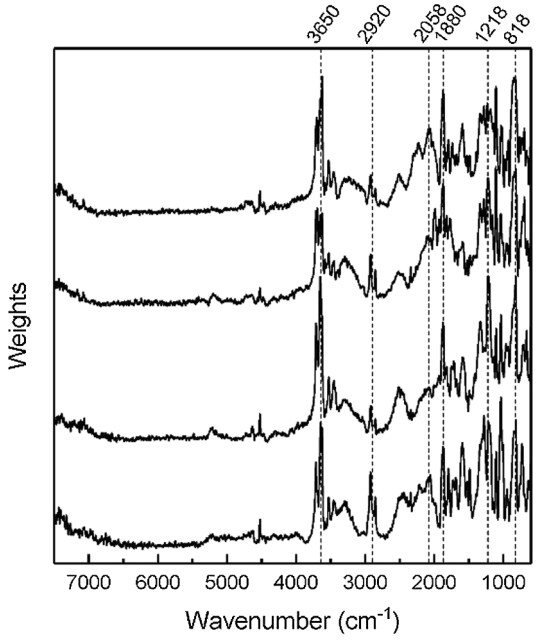

Fig. 3. Maximum weight of each wavenumber in random selections of training iterations ("instance") the hidden layer of an ANN trained to predict POXC from soils in western Kenya (n = 144) using DRIFT spectroscopy.

dataset, and for POXC slightly improved predictions were achieved with ANN. The relatively small sample set of this study even for PLSR-based models do not optimize the hypothesized advantage of ANN for chemometric prediction from large datasets, thus offering a competitive advantage to linear models such as PLSR. Increasing sample size and, or perhaps more importantly, variation in soil properties that translate to spectral diversity (e.g., mineralogy) is expected to enhance the slightly better prediction (RMSE) of POXC by ANN. Our results are consistent with previous PLSR predictions of POXC with moderate to high accuracy (RMSE validation 144 mg kg^{-1}) from two studies differing in an order of magnitude in sample size (n = 24 vs 496) (Calderón et al., 2017; Veum et al., 2014). Of the eight additional soil variables evaluated in this study, the ANN approach showed improvement (lower RMSE) over PLSR in six variables.

However, these improvements were achieved only after careful selection of the ANN to be used and the training hyperparameters. Without significant design space search the ANN performed similarly as PLSR for POXC prediction, but outperformed PLSR for larger pools of SOM (e.g., SOC, C:N) as well as texture fractions. Reduced data complexity to sample size ratio likely explains improved ANN prediction relative to PLSR, because with few training samples it is easier for a neural network to learn from a simpler dataset. However, this does not explain PLSR outperformance of ANN for some soil variables (e.g., bulk density, β-glucosidase activity).

Our study demonstrates that both ANN and PLSR obtain the majority of predictive infrared frequencies for POXC from the MIR compared to NIR, consistent with previous findings (Calderón et al., 2017). Critically, we demonstrate that ANN and PLSR can draw upon different and shared frequencies to produce similar prediction accuracy of the same variable (i.e., POXC). Inspecting component loadings (PLSR) enables attribution of model performance for a particular soil variable to certain wavenumbers (Calderón et al., 2017), and inspection of wavenumbers used in randomly selected instances of the ANN offers an analogous evaluation. Both PLSR and ANN emphasized the phyllosilicate OH region at 3700–3600 cm^{-1}, which may reflect associations of organic matter with minerals. In contrast to the soils analyzed by Calderón et al. (2017) largely being dominated by 2:1 phyllosilicate mineralogy (with the exception being Watkinsville, GA soils), the highly weathered soils in the present study exhibit 1:1 mineralogy (e.g., kaolinite features at 3700 – 3200 cm^{-1}) that was more strongly used by both ANN and PLSR models for POXC prediction. Though indirect, this suggests that POXC composition may be influenced by soil mineralogy (Margenot et al., 2017).

ANN appeared to draw more heavily on wavenumbers corresponding to absorbance of mineral functional groups than of organic functional groups. ANN did not strongly weigh the aliphatic C-H stretch at 3000–2800 cm^{-1}, though previous evaluations have found this spectral feature to be the most strongly and positively correlated to POXC (Calderón et al., 2017; Margenot et al., 2015). Notably, the randomly selected instances of ANN more strongly weighed absorbance at 2050–1800 and 818 cm^{-1} than the aliphatic C-H stretch, absorbances ascribed to quartz-like Si-O (Nguyen et al., 1991; Soda, 1961). Absorbances used by ANN that corresponded to multiple potential organic functional groups with co-contributions to absorbance at 1300–1150 cm^{-1}, including polysaccharide C-O, phenol and carboxyl

C-O, and alcohol O-H (Parikh et al., 2014). All are components of SOM and using assorted non-DRIFT spectroscopic and spectrometric techniques appear related to POXC (Margenot et al., 2017; Romero et al., 2018).

4.2. Designing neural networks in soil spectroscopy

Over the past few years ANN have risen in prominence within the machine learning community. Despite the large body of research on the topic, there has been limited discussion on the in selection of ANN architectures. Several maxims have been developed, but trial and error is still a key component of development. The present study tested over 6000 architecture and hyper-parameter combinations. As such, we feel the reader may benefit from a discussion of the methodology used to select the ANN and hyper-parameters and as well as an overivew of the features of an ANN architecture.

A summary of methodological points on designing and evaluating ANN for soil property prediction from DRIFT spectra of soils are as follows:

(i) As others in the soil community have done (Farifteh et al., 2007; Janik et al., 2009; Kuang et al., 2015; Wijewardane et al., 2016a), it is recommended to keep the number of neurons in layers small. In the present study, using less than 80 neurons appeared to suffice for a network of 1–2 layers and less than 50 for networks with more than two hidden layers, as has been found by others (Janik et al., 2009).

(ii) Given small sample sizes (numbering in the hundreds) a large number of epochs should be used for training (e.g., training epochs in the low hundreds for datasets $n < 1000$).

(iii) Batch sizes should be kept small. Small batch sizes expose networks to risk of overfitting and susceptibility to noise. Training of the ANN should be observed carefully to discover when overfitting begins to occur. It is also imperative with small datasets (again data samples < 1000) that the network learn as much as possible from each data point. With soil spectral datasets typically in the hundreds but increasingly in the thousands or tens of thousands (Nocita et al., 2015), batch sizes should be limited to 1–2.

(iv) Deeper networks (those with more hidden layers) may help increase prediction accuracy. Previous use of ANN for prediction of soil variables (Farifteh et al., 2007; Janik et al., 2009; Kuang et al., 2015; Wijewardane et al., 2016a) tend to use ANN with 1–2 hidden layers. For the present study's dataset, deep networks repeatedly performed better with 5 to 10 layers proving optimal. Soil spectra datasets are likely to increase in size as the increasing availability of high-throughput methods for collecting soil spectra generate large amounts of spectral data (Reeves III et al., 2012) used to populate spectral libraries of regional to global scale (Castaldi et al., 2018; Viscarra Rossel et al., 2016; Wijewardane et al., 2016b). For these larger soil spectral datasets, ANN is likely to offer a more viable alternative to PSLR or other multivariate chemometric models. This is largely due to more limited diversity in soil type and thus soil spectra that generally result from geographically constrained or "local" datasets (Parikh et al., 2014; Sila et al., 2016), PLSR offers good to high performance in prediction soil properties. Larger and/or more geographically extensive soil sample sets that are generally more spectrally diverse datasets may explain why ANN has an additional advantage over PLSR. By virtue of being relatively small ($n = 144$), the sample set used in this study is likely to favor PLSR and thus offers a conservative comparative evaluation of ANN. The need to consider regional and/or soil type-specific soil health indicators (Bongiorno et al., 2019; Bünemann et al., 2018) means that soil sample sets acquired for indicators such as POXC may be more likely to be geographically constrained, further potentially favoring PLSR.

4.3. Software tools and computation resources

ANN can require significant computational power and/or time, with computation scaling linearly with the size of the dataset. For the ANN amodeling in this study, however, we used a desktop computer: a AMD FX 8370 processor with 8 cores, 16 GB of RAM, and two NVIDIA GTX 750 cards. With this setup, training a network over 500 Epochs requires approximately 10 min. Thus, 50 different training-test splits required nearly 9 h of training time using the widely used open-source machine learning framework TensorFlow from Google. TensorFlow represents the state-of-the-art in terms of algorithms and data structures for training large ANN and is available as a software-as-a-service from Google Cloud, which provides a cost-effective way to scale computational resources required on demand. The recent introduction of specialized hardware (e.g., ensor Processing Units (TPUs)) in cloud platforms can significantly accelerate machine learning. This makes using ANN and exploring the design space of the best neural network architecture for a given dataset accessible to both laboratories offering soil spectroscopy as a service and individual researchers who do not have access to significant computational resources.

4.4. Implications for soil health monitoring in agriculture

Quantification of a proposed soil health indicator such as POXC (Hurisso et al., 2018; Moebius-Clune et al., 2016) by DRIFT spectroscopy in this and other studies (Calderón et al., 2017) indicates the possibility of infrared spectroscopy-based assessment of soil health (Veum et al., 2015). Prediction of individual indicators can be accomplished through linear-based methods such as PLSR. For example, microbial biomass C (Reeves III et al., 2012) and mineralizable C (Peltre et al., 2014) as well as more common metrics of total soil C, pH and texture (Parikh et al., 2014) are routinely predicted from DRIFT spectra. The recent emergence of field-deployable, portable FTIR spectrometers (Hutengs et al., 2018; Robertson; Soriano-Disla et al., 2017; Soriano-Disla et al., 2018) raises the possibility of on-site assessment of soil health using chemometric models. The ability of reusing an ANN architecture developed for one variable (e.g., POXC) or other variables (e.g., SOC, clay) as shown in this study raises the possibility of multiply predicting individual soil health indicators from a single ANN model, in contrast to multiple individual indicator-specific PLSR models. Since infrared spectra of soils contain information on soil properties such as texture used to weigh soil health indicators (Mikhailova et al., 2018) and that are predictable from spectra (Parikh et al., 2014), ANN may further enable scoring functions of soil health indicators (Fine et al., 2017) and/or their integration into a final soil health 'score' (Rinot et al., 2019) to be simultaneously calculated.

5. Conclusions

Infrared spectroscopy coupled with chemometrics has enabled cost-effective high-throughput analysis of soil and is increasingly used to upscale spatial and temporal soil property assessment and monitoring. This recent transformation has been driven by the use of linear chemometric models, most notably partial least squares regression (PLSR) to derive soil property measurements or 'predictions' from soil spectra. As soil spectral libraries expand in size concurrent with the scale of soil sampling and mapping efforts to continental and even global coverage, commonly employed linear models such as PLSR may be compromised by the number and diversity of spectra. Artificial neural networks (ANN) have revolutionized numerous scientific and engineering disciplines in recent years by enabling prediction of properties or features from data-rich inputs, making it a promising candidate for chemometric determination of soil properties from infrared spectra. We evaluated the comparative performance of ANN and PLSR to predict routinely measured (e.g., total SOC) and emerging (e.g., permanganate oxidizable C (POXC)) soil properties across a gradient of SOC furnished by a

deforestation chronosequence in Kenya (n = 144). Systematic evaluation of potential ANN architectures was used to identify best-practices for the application of ANN to soil spectroscopy. Additionally, models were assessed for which infrared frequencies were employed using component loadings (PLSR) or randomly selected instances of neuron layers (ANN). Similar or improved predictions by ANN relative to PLSR for standard variables of soil organic matter (SOC, C:N) and physical properties (clay, silt, sand, bulk density) indicates comparable utility of ANN even for smaller spectral datasets thought to favor accuracy of PLSR. Accuracy of POXC predictions were similar for ANN (RMSE 102 mg kg^{-1}) and PLSR (RMSE 106 mg kg^{-1}). That ANN and PLSR models drew on overlapping and distinct wavenumbers in the MIR indicates that these non-linear and linear models, respectively, draw upon different information from soil infrared spectra to derive similar predictions. To help guide future ANN efforts on soil spectra, we propose a systematic procedure to select ANN model hyperparameters.

Declaration of Competing Interest

The authors declare that they have no known competing financial interests or personal relationships that could have appeared to influence the work reported in this paper.

Acknowledgements

This work was supported in part by funding from the German Federal Ministry for Economic Cooperation and Development (BMZ)/ Deutsche Gesellschaft für Internationale Zusammenarbeit (GIZ) under contract # 81194110. We thank John Mukalama and other CIAT staff for field assistance.

Appendix A. Supplementary material

Supplementary data to this article can be found online at https://doi.org/10.1016/j.compag.2019.105098.

References

Abadi, M., Barham, P., Chen, J., Chen, Z., Davis, A., Dean, J., Devin, M., Ghemawat, S., Irving, G., Isard, M., 2016. Tensorflow: a system for large-scale machine learning. OSDI 265–283.

Bagheri Bodaghabadi, M., MartÍNez-Casasnovas, J., Salehi, M.H., Mohammadi, J., Esfandiarpoor Borujeni, I., Toomanian, N., Gandomkar, A., 2015. Digital soil mapping using artificial neural networks and terrain-related attributes. Pedosphere 25, 580–591.

Bellon-Maurel, V., Fernandez-Ahumada, E., Palagos, B., Roger, J.-M., McBratney, A., 2010. Critical review of chemometric indicators commonly used for assessing the quality of the prediction of soil attributes by NIR spectroscopy. TrAC. Trends Anal. Chem. 29, 1073–1081.

Berazneva, J., McBride, L., Sheahan, M., Güereña, D., 2018. Empirical assessment of subjective and objective soil fertility metrics in east Africa: implications for researchers and policy makers. World Dev. 105, 367–382.

Bongiorno, G., Bünemann, E.K., Oguejiofor, C.U., Meier, J., Gort, G., Comans, R., Mäder, P., Brussaard, L., de Goede, R., 2019. Sensitivity of labile carbon fractions to tillage and organic matter management and their potential as comprehensive soil quality indicators across pedoclimatic conditions in Europe. Ecol. Ind. 99, 38–50.

Bünemann, E.K., Bongiorno, G., Bai, Z., Creamer, R.E., De Deyn, G., de Goede, R., Fleskens, L., Geissen, V., Kuyper, T.W., Mäder, P., Pulleman, M., Sukkel, W., van Groenigen, J.W., Brussaard, L., 2018. Soil quality – a critical review. Soil Biol. Biochem. 120, 105–125.

Calderón, F.J., Culman, S., Six, J., Franzluebbers, A.J., Schipanski, M., Beniston, J., Grandy, S., Kong, A.Y.Y., 2017. Quantification of soil permanganate oxidizable C (POXC) using infrared spectroscopy. Soil Sci. Soc. Am. J. 81, 277–288.

Castaldi, F., Chabrillat, S., Chartin, C., Genot, V., Jones, A.R., van Wesemael, B., 2018. Estimation of soil organic carbon in arable soil in Belgium and Luxembourg with the LUCAS topsoil database. Eur. J. Soil Sci.

Chollet, F., 2015. keras. GitHub (2015).

Culman, S.W., Snapp, S.S., Freeman, M.A., Schipanski, M.E., Beniston, J., Lal, R., Drinkwater, L.E., Franzluebbers, A.J., Glover, J.D., Grandy, A.S., Lee, J., Six, J., Maul, J.E., Mirksy, S.B., Spargo, J.T., Wander, M.M., 2012. Permanganate oxidizable carbon reflects a processed soil fraction that is sensitive to management. Soil Sci. Soc. Am. J. 76, 494–504.

Farifteh, J., Van der Meer, F., Atzberger, C., Carranza, E.J.M., 2007. Quantitative analysis of salt-affected soil reflectance spectra: a comparison of two adaptive methods (PLSR and ANN). Remote Sens. Environ. 110, 59–78.

Fine, A.K., van Es, H.M., Schindelbeck, R.R., 2017. Statistics, scoring functions, and regional analysis of a comprehensive soil health database. Soil Sci. Soc. Am. J. 81, 589–601.

Guillou, F.L., Wetterlind, W., Viscarra Rossel, R.A., Hicks, W., Grundy, M., Tuomi, S., 2015. How does grinding affect the mid-infrared spectra of soil and their multivariate calibrations to texture and organic carbon? Soil Res. 53, 913–921.

Hurisso, T.T., Culman, S.W., Horwath, W.R., Wade, J., Cass, D., Beniston, J.W., Bowles, T.M., Grandy, A.S., Franzluebbers, A.J., Schipanski, M.E., Lucas, S.T., Ugarte, C.M., 2016. Comparison of permanganate-oxidizable carbon and mineralizable carbon for assessment of organic matter stabilization and mineralization. Soil Sci. Soc. Am. J. 80, 1352–1364.

Hurisso, T.T., Culman, S.W., Zhao, K., 2018. Repeatability and spatiotemporal variability of emerging soil health indicators relative to routine soil nutrient tests. Soil Sci. Soc. Am. J. 82, 939–948.

Hutengs, C., Ludwig, B., Jung, A., Eisele, A., Vohland, M., 2018. Comparison of portable and bench-top spectrometers for mid-infrared diffuse reflectance measurements of soils. Sensors 18, 993.

Janik, L.J., Forrester, S.T., Rawson, A., 2009. The prediction of soil chemical and physical properties from mid-infrared spectroscopy and combined partial least-squares regression and neural networks (PLS-NN) analysis. Chemometr. Intellig. Lab. Syst. 97, 179–188.

Kuang, B., Tekin, Y., Mouazen, A.M., 2015. Comparison between artificial neural network and partial least squares for on-line visible and near infrared spectroscopy measurement of soil organic carbon, pH and clay content. Soil Tillage Res. 146, 243–252.

Lehmann, J., Kinyangi, J., Solomon, D., 2007. Organic matter stabilization in soil microaggregates: implications from spatial heterogeneity of organic carbon contents and carbon forms. Biogeochemistry 85, 45–57.

Liu, L., Ji, M., Buchroithner, M., 2018. Transfer learning for soil spectroscopy based on convolutional neural networks and its application in soil clay content mapping using hyperspectral imagery. Sensors 18, 3169.

Liu, W., Wang, Z., Liu, X., Zeng, N., Liu, Y., Alsaadi, F.E., 2017. A survey of deep neural network architectures and their applications. Neurocomputing 234, 11–26.

Lucas, S.T., Weil, R.R., 2012. Can a labile carbon test be used to predict crop responses to improve soil organic matter management? Agron. J. 104, 1160–1170.

Margenot, A.J., Calderón, F.J., Bowles, T.M., Parikh, S.J., Jackson, L.E., 2015. Soil organic matter functional group composition in relation to organic carbon, nitrogen, and phosphorus fractions in organically managed tomato fields. Soil Sci. Soc. Am. J. 79, 772–782.

Margenot, A.J., Calderón, F.J., Magrini, K.A., Evans, R.J., 2017. Application of DRIFTS, 13C NMR, and py-MBMS to characterize the effects of soil science oxidation assays on soil organic matter composition in a mollic xerofluvent. Appl. Spectrosc. 71, 1506–1518.

Mikhailova, E.A., Post, C.J., Schlautman, M.A., Galbraith, J.M., Zurqani, H.A., 2018. Usability of soil survey soil texture data for soil health indicator scoring. Commun. Soil Sci. Plant Anal. 49, 1826–1834.

Moebius-Clune, B.N., D.J. Moebius-Clune, Gugino, B.K., Idowu, O.J., Schindelbeck, R.R., Ristow, A.J., Es, H.M.v., Thies, J.E., Shayler, H.A., McBride, M.B., Wolfe, D.W., 2016., G.S.A., 2016. Comprehensive assessment of soil health–Cornell Framework Manual. 3.1. ed. Cornell University Geneva, NY.

Morellos, A., Pantazi, X.-E., Moshou, D., Alexandridis, T., Whetton, R., Tziotzios, G., Wiebensohn, J., Bill, R., Mouazen, A.M., 2016. Machine learning based prediction of soil total nitrogen, organic carbon and moisture content by using VIS-NIR spectroscopy. Biosyst. Eng. 152, 104–116.

Mouazen, A.M., Kuang, B., De Baerdemaeker, J., Ramon, H., 2010. Comparison among principal component, partial least squares and back propagation neural network analyses for accuracy of measurement of selected soil properties with visible and near infrared spectroscopy. Geoderma 158, 23–31.

Nanni, M.R., Cezar, E., Silva Junior, C.A.d., Silva, G.F.C., da Silva Gualberto, A.A., 2018. Partial least squares regression (PLSR) associated with spectral response to predict soil attributes in transitional lithologies. Archives of Agronomy and Soil Science 64, 682-695.

Nguyen, T., Janik, L.J., Raupach, M., 1991. Diffuse reflectance infrared Fourier transform (DRIFT) spectroscopy in soil studies. Soil Res. 29, 49–67.

Nocita, M., Stevens, A., van Wesemael, B., Brown, D.J., Shepherd, K.D., Towett, E., Vargas, R., Montanarella, L., 2015. Soil spectroscopy: an opportunity to be seized. Glob. Change Biol. 21, 10–11.

NRCS, 2019. Recommended Soil Health Indicators and Associated Laboratory Procedures, In: Stott, D.E. (Ed.), Soil Health. USDA NRCS, Washington, D.C.

Parikh, S.J., Goyne, K.W., Margenot, A.J., Mukome, F.N.D., Calderón, F.J., 2014. Chapter One - Soil Chemical Insights Provided through Vibrational Spectroscopy. In: Donald, L.S. (Ed.), Advances in Agronomy. Academic Press, pp. 1–148.

Paul, B.K., Vanlauwe, B., Ayuke, F., Gassner, A., Hoogmoed, M., Hurisso, T.T., Koala, S., Lelei, D., Ndabamenye, T., Six, J., Pulleman, M.M., 2013. Medium-term impact of tillage and residue management on soil aggregate stability, soil carbon and crop productivity. Agric. Ecosyst. Environ. 164, 14–22.

Pedregosa, F., Varoquaux, G., Gramfort, A., Michel, V., Thirion, B., Grisel, O., Blondel, M., Prettenhofer, P., Weiss, R., Dubourg, V., 2011. Scikit-learn: machine learning in python. J. Mach. Learn. Res. 12, 2825–2830.

Peltre, C., Bruun, S., Du, C., Thomsen, I.K., Jensen, L.S., 2014. Assessing soil constituents and labile soil organic carbon by mid-infrared photoacoustic spectroscopy. Soil Biol. Biochem. 77, 41–50.

Real, E., Moore, S., Selle, A., Saxena, S., Suematsu, Y.L., Tan, J., Le, Q., Kurakin, A., 2017. Large-scale evolution of image classifiers. arXiv preprint arXiv:1703.01041.

Reeves III, J.B., McCarty, G.W., Calderon, F., Hively, W.D., 2012. Chapter 20 - Advances in Spectroscopic Methods for Quantifying Soil Carbon. In: Franzluebbers, A.J.,

Follett, R.F. (Eds.), Managing Agricultural Greenhouse Gases. Academic Press, San Diego, pp. 345–366.
Reeves III, J.B., Smith, D.B., 2009. The potential of mid- and near-infrared diffuse reflectance spectroscopy for determining major- and trace-element concentrations in soils from a geochemical survey of North America. Appl. Geochem. 24, 1472–1481.
Rinot, O., Levy, G.J., Steinberger, Y., Svoray, T., Eshel, G., 2019. Soil health assessment: a critical review of current methodologies and a proposed new approach. Sci. Total Environ. 648, 1484–1491.
Robertson, A.J., Hill, H.R., Main, A.M., Analysis of soil in the field using portable FTIR.
Roggo, Y., Chalus, P., Maurer, L., Lema-Martinez, C., Edmond, A., Jent, N., 2007. A review of near infrared spectroscopy and chemometrics in pharmaceutical technologies. J. Pharm. Biomed. Anal. 44, 683–700.
Romero, C.M., Engel, R.E., D'Andrilli, J., Chen, C., Zabinski, C., Miller, P.R., Wallander, R., 2018. Patterns of change in permanganate oxidizable soil organic matter from semiarid drylands reflected by absorbance spectroscopy and Fourier transform ion cyclotron resonance mass spectrometry. Org Geochem. 120, 19–30.
Rossel, R.A.V., Behrens, T., 2010. Using data mining to model and interpret soil diffuse reflectance spectra. Geoderma 158, 46–54.
Sanchez, P.A., Ahamed, S., Carré, F., Hartemink, A.E., Hempel, J., Huising, J., Lagacherie, P., McBratney, A.B., McKenzie, N.J., Mendonça-Santos, M.d.L., Minasny, B., Montanarella, L., Okoth, P., Palm, C.A., Sachs, J.D., Shepherd, K.D., Vågen, T.-G., Vanlauwe, B., Walsh, M.G., Winowiecki, L.A., Zhang, G.-L., 2009. Digital Soil Map of the World. Science 325, 680-681.
Schindelbeck, R.R., B.N. Moebius-Clune, Moebius-Clune, D.J., Kurtz, K.S., Es, H.M.v., 2016. Cornell Soil Health Laboratory: Comprehensive assessment of soil health standard operating procedures. Cornell University, Geneva, NY.
Shepherd, K.D., Vanlauwe, B., Gachengo, C.N., Palm, C.A., 2005. Decomposition and mineralization of organic residues predicted using near infrared spectroscopy. Plant Soil 277, 315–333.
SHI, 2017. Enriching Soil, Enhancing Life: An Action Plan for Soil Health, In: Honeycutt, C.W. (Ed.). Soil Health Institute, p. 48.
Sila, A.M., Shepherd, K.D., Pokhariyal, G.P., 2016. Evaluating the utility of mid-infrared spectral subspaces for predicting soil properties. Chemometr. Intell. Lab. Syst. 153, 92–105.
Soda, R., 1961. Infrared absorption spectra of quartz and some other silica modification. Bull. Chem. Soc. Jpn. 34, 1491–1495.
Solomon, D., Lehmann, J., Kinyangi, J., Amelung, W., Lobe, I., Pell, A., Riha, S., Ngoze, S., Verchot, L.O.U., Mbugua, D., Skjemstad, J.A.N., SchÄFer, T., 2007. Long-term impacts of anthropogenic perturbations on dynamics and speciation of organic carbon in tropical forest and subtropical grassland ecosystems. Glob. Change Biol. 13, 511–530.
Soriano-Disla, J.M., Janik, L.J., Allen, D.J., McLaughlin, M.J., 2017. Evaluation of the performance of portable visible-infrared instruments for the prediction of soil properties. Biosyst. Eng. 161, 24–36.
Soriano-Disla, J.M., Janik, L.J., McLaughlin, M.J., 2018. Assessment of cyanide contamination in soils with a handheld mid-infrared spectrometer. Talanta 178, 400–409.
Stevens, A., Nocita, M., Tóth, G., Montanarella, L., van Wesemael, B., 2013. Prediction of soil organic carbon at the european scale by visible and near infrared reflectance spectroscopy. PLoS ONE 8, e66409.
Stumpe, B., Weihermüller, L., Marschner, B., 2011. Sample preparation and selection for qualitative and quantitative analyses of soil organic carbon with mid-infrared reflectance spectroscopy. Eur. J. Soil Sci. 62, 849–862.
Szegedy, C., Liu, W., Jia, Y., Sermanet, P., Reed, S., Anguelov, D., Erhan, D., Vanhoucke, V., Rabinovich, A., 2015. Going deeper with convolutions. In: Proceedings of the IEEE conference on computer vision and pattern recognition, pp. 1–9.
Tange, R.I., Rasmussen, M.A., Taira, E., Bro, R., 2017. Benchmarking support vector regression against partial least squares regression and artificial neural network: effect of sample size on model performance. J. Near Infrared Spectrosc. 25, 381–390.
Towett, E.K., Shepherd, K.D., Sila, A., Aynekulu, E., Cadisch, G., 2015. Mid-infrared and total X-ray fluorescence spectroscopy complementarity for assessment of soil properties. Soil Sci. Soc. Am. J. 79, 1375–1385.
Veum, K., Goyne, K., Kremer, R., Miles, R., Sudduth, K., 2014. Biological indicators of soil quality and soil organic matter characteristics in an agricultural management continuum. Biogeochemistry 117, 81–99.
Veum, K.S., Sudduth, K.A., Kremer, R.J., Kitchen, N.R., 2015. Estimating a soil quality index with VNIR reflectance spectroscopy. Soil Sci. Soc. Am. J. 79, 637–649.
Viscarra Rossel, R.A., Behrens, T., Ben-Dor, E., Brown, D.J., Demattê, J.A.M., Shepherd, K.D., Shi, Z., Stenberg, B., Stevens, A., Adamchuk, V., Aïchi, H., Barthès, B.G., Bartholomeus, H.M., Bayer, A.D., Bernoux, M., Böttcher, K., Brodský, L., Du, C.W., Chappell, A., Fouad, Y., Genot, V., Gomez, C., Grunwald, S., Gubler, A., Guerrero, C., Hedley, C.B., Knadel, M., Morrás, H.J.M., Nocita, M., Ramirez-Lopez, L., Roudier, P., Campos, E.M.R., Sanborn, P., Sellitto, V.M., Sudduth, K.A., Rawlins, B.G., Walter, C., Winowiecki, L.A., Hong, S.Y., Ji, W., 2016. A global spectral library to characterize the world's soil. Earth Sci. Rev. 155, 198–230.
Viscarra Rossel, R.A., Walvoort, D.J.J., McBratney, A.B., Janik, L.J., Skjemstad, J.O., 2006. Visible, near infrared, mid infrared or combined diffuse reflectance spectroscopy for simultaneous assessment of various soil properties. Geoderma 131, 59–75.
Weil, R.R., Islam, K.R., Stine, M.A., Gruver, J.B., Samson-Liebig, S.E., 2003. Estimating active carbon for soil quality assessment: a simplified method for laboratory and field use. Am. J. Altern. Agric. 18, 3–17.
Were, K., Bui, D.T., Dick, Ø.B., Singh, B.R., 2015. A comparative assessment of support vector regression, artificial neural networks, and random forests for predicting and mapping soil organic carbon stocks across an Afromontane landscape. Ecol. Ind. 52, 394–403.
Wijewardane, N.K., Ge, Y., Morgan, C.L.S., 2016a. Moisture insensitive prediction of soil properties from VNIR reflectance spectra based on external parameter orthogonalization. Geoderma 267, 92–101.
Wijewardane, N.K., Ge, Y., Wills, S., Loecke, T., 2016b. Prediction of soil carbon in the conterminous united states: visible and near infrared reflectance spectroscopy analysis of the rapid carbon assessment project. Soil Sci. Soc. Am. J. 80, 973–982.
Xie, H., Zhao, J., Wang, Q., Sui, Y., Wang, J., Yang, X., Zhang, X., Liang, C., 2015. Soil type recognition as improved by genetic algorithm-based variable selection using near infrared spectroscopy and partial least squares discriminant analysis. Sci. Rep. 5, 10930.
Yeasmin, S., Singh, B., Johnston, C.T., Sparks, D.L., 2017. Evaluation of pre-treatment procedures for improved interpretation of mid infrared spectra of soil organic matter. Geoderma 304, 83–92.
Zhang, L., Yang, X., Drury, C., Chantigny, M., Gregorich, E., Miller, J., Bittman, S., Reynolds, D., Yang, J., 2017. Infrared spectroscopy prediction of organic carbon and total nitrogen in soil and particulate organic matter from diverse Canadian agricultural regions. Can. J. Soil Sci. 98, 77–90.
Zhao, S.J., Zhang, J., Xu, Y.M., Xiong, Z.H., 2006. Nonlinear projection to latent structures method and its applications. Ind. Eng. Chem. Res. 45, 3843–3852.